Submicrometer-Sized ZIF-71 Filled Organophilic Membranes for Improved Bioethanol Recovery: Mechanistic Insights by Monte Carlo Simulation and FTIR Spectroscopy

(Article begins on next page)

15 October 2023

UNIVERSITÀ DEGLI STUDI DI TORINO

Abstract

Template-free self-assembly synthesis of nano-sized metal-organic frameworks (MOFs) is of particular interest in MOF research since organized nanostructures possessing distinctive properties are useful for many advanced applications. In this work, the facile room temperature synthesis of robust submicrometer-sized ZIF-71 crystals with different particle sizes (140, 290, or 430 nm), having a high permanent microporosity (S BET = 827 cm 2 g −1) and synthesis yield up to 80% based on Zn on a gram-scale, is reported. These small ZIF-71 particles are ideal fi ller for the fabrication of thinner and homogeneous polydimethylsiloxane (PDMS) based mixed matrix membranes (MMMs) with excellent fi ller dispersion and fi ller-polymer adhesion at high loading up to 40 wt%, as confi rmed by scanning electron microscopy. Pervaporation tests using these submicrometer-sized ZIF-71 fi lled MMMs show signifi cant improvement for bioethanol recovery. Interesting phenomena of i) reversible ethanol-ethanol hydrogen interaction in the ethanol liquidphase and ii) irreversible hydrogen interaction of ethanol and –Cl functional group in the α-cages and octagonal prismatic cages of ZIF 71 in ethanol vapor-phase are discovered for the fi rst time by a Fourier transform infrared spectroscopy (FTIR) study. In full agreement with molecular simulation results, these explain fundamentally the ZIF-71 fi lled MMMs pervaporation performance.

1 Introduction

Metal-organic frameworks (MOFs) are crystalline porous materials composed of inorganic moieties and organic ligand bridges.[1] The versatility of both inorganic units and organic linkers offers a toolbox[1b,c] for creating MOFs with diversified framework topologies, chemical functionalities, tunable pore sizes and large surface areas suited for a vast range of potential applications such as gas storage/separation,[2] catalysis,[3] sensing,[4] and drug delivery.[5]

For many targeted applications, downsizing the MOF particles is highly desirable in order to maximize the expression of intrinsic properties. For example, nano-sized MOFs have been demonstrated to be a promising platform for drug delivery and bioimaging.[5] MOF nanoparticles with enhanced accessibility to the interior and high external specific surface area have shown significant improvement in liquid phase catalysis.[6] Controlling size and shape of nanocrystals is also an important element for the optimization of thin films/membranes with respect to grain boundaries, leakage and thickness.[7] For these reasons, nano-sized MOFs are increasingly attracting the attention of the MOF research community.[8] Reported techniques for the synthesis of MOF nanoparticles include modulated/surfactant-mediated synthesis,[9] microwave heating,[10] mechanochemical,[11] low temperature synthesis,[12] concentrated synthesis[13] and solvent precipitation approaches.[14]

Zeolitic imidazolate frameworks (ZIFs) are a subclass of MOFs constructed from tetrahedral Zn metal ions and imidazolate linkers.[15] Owing to their intrinsic hydrophobicity, and superior thermal and chemical stability among the reported MOFs. ZIFs or ZIFs-base membranes (e.g., ZIF-7, ZIF-8, ZIF-69, ZIF-71, and ZIF-90) are attractive candidates for gas adsorption and molecular separation.[16, 17] Nair and co-workers were first to synthesize uniform and well-defined submicrometer ZIF-90 crystals for the fabrication of MMMs which showed remarkable improvement in both CO2 permeability and CO2/CH4 or CO2/CH4 selectivity.[17b],[17c] Recently, the development of ZIF containing membranes for liquid phase separation has been reported.[18] For example, Yang and co-workers[18b] reported the recovery of biobutanol via pervaporation using ZIF-8 filled PMPS (polymethylphenylsiloxane) MMMs. Very recently, Zhang and co-workers[18f] reported the spray self-assembly fabrication of hybrid MMMs with 40 wt% ZIF-8 loading for efficient biobutanol recovery from aqueous solution. Dong and Lin[18c] demonstrated the successful growth of a ZIF-71 membrane on a ZnO support via secondary growth and its use in the pervaporation of methanol-water mixtures. A relatively thick membrane (10 μm) composed of large micro¬meter-sized ZIF-71 crystals was obtained. Although ZIF-71 based membranes have shown molecular sieving effect for bio-alcohol separation, both the size and uniformity of the ZIF-71 nanoparticles as well as their homogeneous dispersion in a polymer matrix remain to be improved in order to enhance pervaporation performance in bioalcohol recovery from

aqueous solution under mild feeding conditions. Due to the lack of preparation techniques, the most available nano-version of ZIFs is limited to ZIF-8[19] and only a few reports on ZIF-7,[20] ZIF-71,[21] ZIF-67,[22] and ZIF-90.[23]. Recently, micrometer-sized ZIF-71 based MMMs have been prepared and evaluated for the recovery of bioethanol and biobutanol via pervaporation.[18d],[18g] Herein, we present an attractive procedure for the synthesis of submicrometer-sized ZIF-71 via a mixed-solvent approach at room temperature. These submicrometer-sized ZIF-71 crystals were excellent fillers to prepare thinner, smooth and homogeneous MMMs, useful for improving the pervaporation performance in ethanol-water mixtures. The interaction of ethanol in the cages of ZIF-71 was examined by in-depth FTIR spectroscopy and molecular simulation providing microscopic insight into the adsorption mechanism of ethanol and water. The FTIR and simulation results revealed the significant influence of linker functional group, pressure and ethanol concentration in ethanol/water adsorption behavior in the α-cages and octagonal prismatic cages of ZIF-71 on the selectivity of the ZIF-71 filled MMMs.

2 Results and Discussion

2.1 Characterization of Submicrometer-Sized ZIF-71

The as-synthesized ZIF-71 from methanol/DMF mixture has a uniform particle size around 290 nm according to SEM (Figure 1c,d), which was smaller than the ZIF-71 crystals (1–2 μm) prepared in methanol solvent (Figure 1a,b). The hydrodynamic diameter of the as-synthesized ZIF-71 crystal was ca. 290 nm with a mono-modal particle size distribution according to DLS analysis (Figure 2a). Moreover, the colloidal suspension of ZIF-71 in the methanol:DMF synthesis solution is stable at room temperature for 24 h (Figure 3a). Wiebcke and co-workers[21a] reported the synthesis of nanosized (30–60 nm) ZIF-71 using 1-propanol as a solvent. These nanosized ZIF-71 were found as an intermediate phase obtained after 5 min and after a prolonged synthesis time to 24 h, a new SOD polymorph was obtained. Very recently, Chung and co-workers[21b] reported the synthesis of 100 nanometer-sized ZIF-71 from DMF solution in an excess of dcIm linker. The use of excess linker is an efficient way of controlling the particle size at a nanometer scale via stabilization of the early MOF nucleates first reported by Cravillion et al.[19a] The mixed solvent synthesis protocol demonstrated in this study is highly reproducible and could be easily scaled up to 1 g/batch for the fabrication of MMMs as demonstrated as a proof of concept the importance of particle size filler for improving membrane performance in bioethanol recovery (vide infra Section 'SEM Investigation of ZIF-71 Filled MMMs').
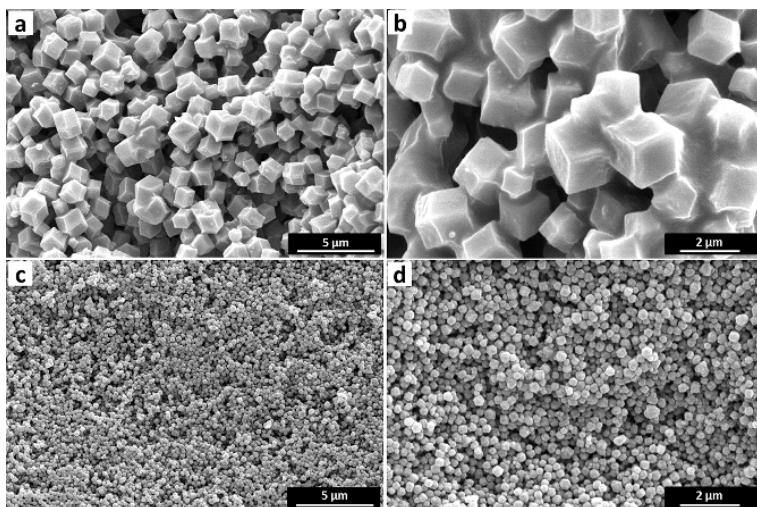

Figure 1. SEM images of a,b) micrometer-sized ZIF-71 prepared in methanol solvent and c,d) submicrometer-sized ZIF-71 crystals prepared in methanol:DMF mixed solvents viewed at different magnifications.
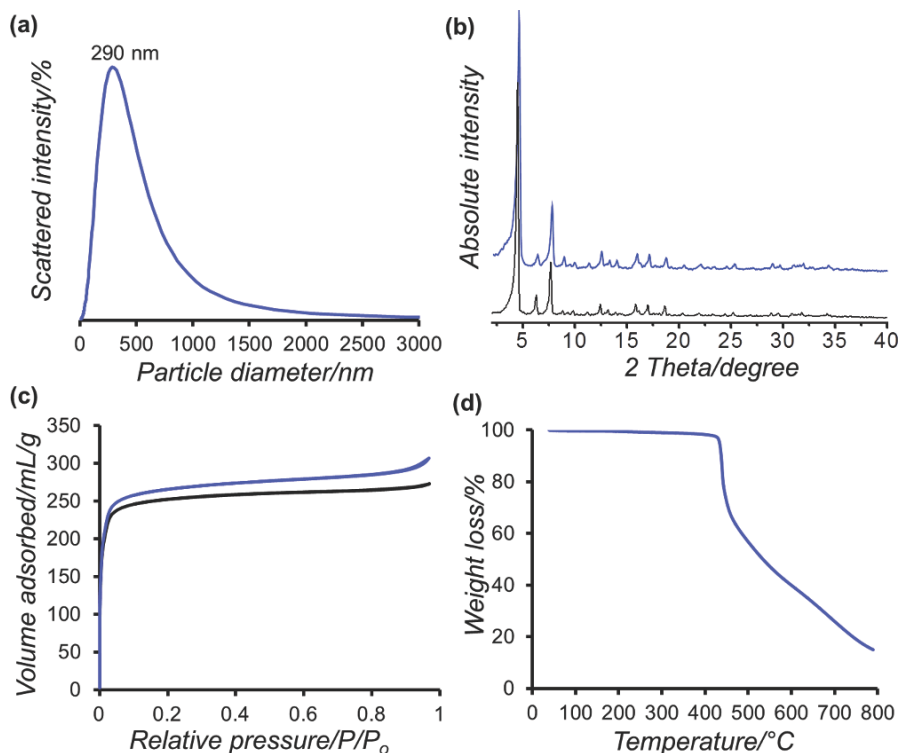
Figure2.Characterization of micrometer-sized (black) and submicrometer-sized (blue) ZIF-71 crystals by a) DLS, b) XRD, c) N_2 physisorption, and d) TGA.
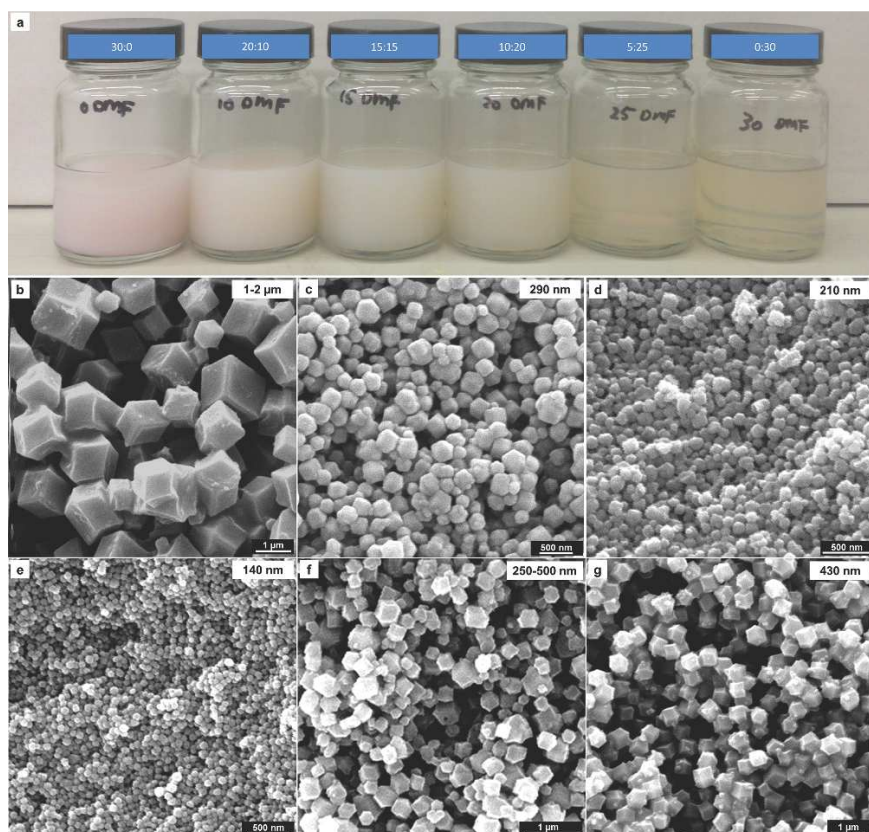
Figure3. The influence of methanol:DMF mixed solvents on the crystallization kinetic of ZIF-71 synthesis. a) Photograph of a series of methanol:DMF mixed solvents synthesis solutions taken after 30 min at room temperature and the corresponding b–f) SEM images of recovered ZIF-71 crystals. Volume ratios of methanol:DMF. b) 30:0, c) 20:10, d) 15:15, e) 10:20, f) 5:25, and g) 0:30.

Phase purity and crystallinity of the as-synthesized submicrometer-sized ZIF-71 sample were verified by XRD (Figure 2b). The N2 physisorption analysis reveals Type I isotherm with a strong uptake at low relative pressure and a plateau (Figure 2c), which is the typical characteristic of a microporous material.[24] The calculated specific BET surface area, Langmuir surface area and micropore volume were 827 m2 g−1, 1148 m2 g−1, and 0.41 cm3 g−1, respectively. TG analysis performed under nitrogen atmosphere (Figure 3d) showed a negligible weight loss between 50–200 °C, indicating the hydrophobic behavior of ZIF-71. The material decomposes at 415 °C.

2.2 Influence of Solvent on Particle Size, Morphology, and Synthesis Yield

ZIF-71 could be synthesized using either DMF or methanol as solvent.[25] It was observed that the crystallization kinetic of ZIF-71 changes dramatically in the methanol:DMF mixed solvents system as shown in the Figure 3a. The observed effect is more likely to be caused by a stronger solvation of the Zn(II) ion by DMF, possibly enhanced by solvation of the ligand.[26] The effect of solvent on the particle size, morphology and synthesis yield was further investigated. A series of 6 synthesis solutions containing different ratios of methanol:DMF (v/v) were prepared: 30:0, 25:5, 20:10, 15:15, 10:20, and 0.30 and their influences on the particle sizes of ZIF-71 are presented in Figure 3b–g. The total volume of the synthesis mixture was 30 mL. ZIF-71 synthesized from methanol solvent produced micrometer-sized crystals of 1–2 μm with a rhombic dodecahedron morphology (Figure 3b).[27] Interestingly, reducing the volume of methanol by 10 mL and replaced with DMF, smaller crystals of 290 nm having the rhombic dodecahedron with truncated corners morphology were obtained as shown in Figure 3c.[27] Increasing the DMF volume from 10 to 20 mL, the particle size of the ZIF-71 crystals decreases to about 140 nm in diameter according to SEM imaging (Figure 3f). Upon increasing the DMF content to 25 mL, ZIF-71 crystal increased slightly to 250–500 nm as shown in Figure 3g. The ZIF-71 crystals morphology was transformed back from rhombic dodecahedron with truncated corners to rhombic dodecahedron shaped. In the synthesis solution containing only DMF, ZIF-71 with a larger particle size of about 430 nm was obtained.

In the present system, the rate of nucleation and crystal growth were significantly affected by the rate of deprotonation of organic linkers to hinder the supramolecular coordination interaction between the inorganic Zn(II) ions and dcIm ligands, resulting in fine tuning of ZIF-71 crystals size and morphology. The introduction of a small amount of DMF into the synthesis solution reduces the association effects between linker molecules, accelerating the rates of deprotonation and nucleation, thus decreasing the ZIF-71 crystal size in width. Increasing the DMF content, its dispersive action became much more prominent. As a result, 140 nm sized ZIF-71 crystals were obtained. On the other hand, in the synthesis system containing only DMF, the deprotonation rate of the dcIm linkers was reduced and thus decreasing the availability of deprotonated linker for coordination and promoting crystal growth, which leads to larger ZIF-71 crystal of about 430 nm. The influence of DMF solvent on the crystallization kinetic for ZIF-71 synthesis at room temperature in the absence of surfactant/modulator is of paramount important serving as a clear precursor solution for direct MOF patterning/printing for future microelectronic applications.[28]

The influence of mixed solvent system on the reaction processes and crystallization kinetics were further studied by measuring the pH values as summarized in Figure 4. The introduction of DMF (15–20 mL) to methanol, the pH of the reaction mixture decreases from 5.6 to 5.3, indicating that more deprotonated dcIm are available for coordination with Zn (II) ions, resulting in nucleation. As a result, smaller crystal size (140–210 nm, Figure 3c,d) was obtained. As the DMF content continues to increase, the pH of the reaction mixtures starts to rise to 7.9. The increase of pH could be due to lower deprotonation rate of the dcIm linker leading to the formation of larger crystals size (430 nm). The influence of pH changes corresponds to the volume ratio of methanol:DMF mixed solvents to the ZIF-71 crystal sizes were in full agreement with the SEM results (Figure 3). It was observed that the variation tendency of pH has an inverse linear relationship to the synthesis yield

as presented in Figure 4. With increasing DMF content, a significant amount of remaining unreacted dcIm linkers resulting in lower yield 51% based on Zn for the synthesis system when DMF is the only solvent used. Nevertheless, a considerable high synthesis yield was obtained for 290 nm sized ZIF-71 crystals (80%) comparable to the micrometer-sized ZIF-71 synthesized from original methanol solvent (84%) (Figure 4).
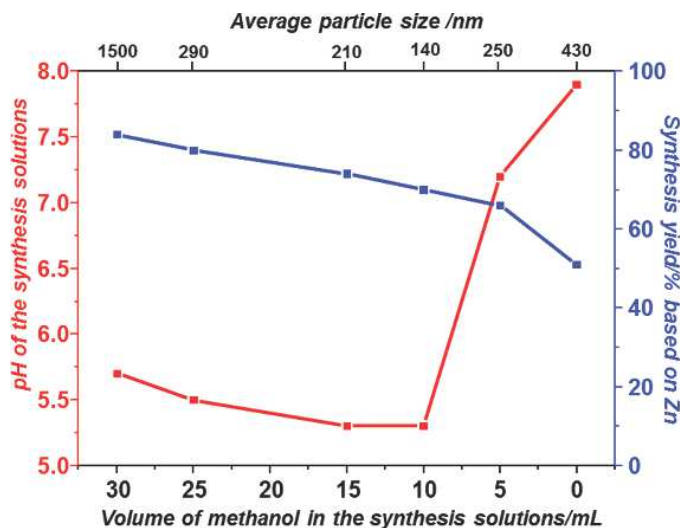

Figure4. Influence of methanol:DMF volume ratios on the pH of the synthesis solution (axis-Y_1) and the corresponding synthesis yield (axis-Y_2).

2.3 SEM Investigation of ZIF-71 Filled MMMs

ZIF-71 is a three-dimensional porous material with accessible cages of 1.68 nm interconnected through small windows of 0.48 nm.[25] ZIF-71 belongs to the RHO type family where the dcIm linkers are dual-functionalized at positions 4 and 5. The 4, 6, and 8-membered rings are interconnected to form truncated cubo-octahedra (α-cages) in a cubic body-centered arrangement. A recent molecular simulation suggests that ZIF-71 could selectively adsorb ethanol from aqueous solution.[25a] To verify this prediction, MMMs were prepared for pervaporation testing using the 290 nm submicrometer-sized ZIF-71 crystals owing to its high synthesis yield (80%) and uniform crystal size. Figure 5 shows the top and cross-sectional SEM images of 20 wt% ZIF-71 filled PDMS membranes cast from a 4% solution of PDMS in hexane. The top views SEM images (Figure 5b) show that the membranes synthesized using these submicro¬meter-sized ZIF-71 crystals were smooth and homogeneous. The submicrometer-sized crystals were completely covered with PDMS in sharp contrast to the MMMs prepared from micrometer-sized ZIF-71 crystals (Figure 5a) where defects are observed allover. Cross-sectional SEM images (Figure 5d) revealed that the submicrometer-sized ZIF-71 filled PDMS membrane had a uniform thickness of 2.8 μm. The submicrometer-sized ZIF-71 crystals were homogeneously dispersed in the PDMS matrix. No interfacial voids nor particle agglomerations were observed. On the other hand, the micrometer-sized ZIF-71 filled membranes (Figure 5c) were rough and uneven with large interstitial voids (Figure 5a). The discrepancies confirm the importance of filler particle size for the preparation of high quality membranes.
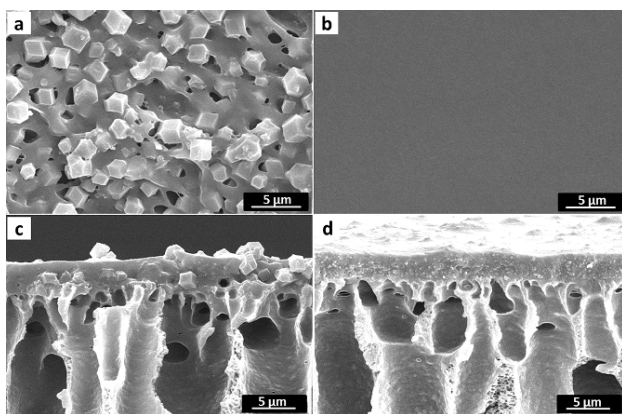
Figure 5. Comparison of a,b) top and c,d) cross-sectional views SEM images of a,c) micrometer-sized and b,d) submicrometer-sized loaded ZIF-71 MMMs prepared from 4% PDMS in hexane with 20 wt% MOF loading.

In another series of experiments, ZIF-71 PDMS membranes filled with different ZIF-71 loadings (20, 30, 40 wt%) were prepared from 20% polymer solutions. The top and cross-sectional views SEM images of submicrometer-sized and micrometer-sized ZIF-71 PDMS membranes are depicted in Figure 6 and Supporting Information Figure S1, respectively. Using the submicrometer-sized ZIF-71, no large clusters nor aggregates of ZIF-71 particles were observed in SEM. Even at higher loadings of ZIF-71 (40 wt%), the MMMs appeared to be smooth with excellent ZIF-71 dispersion. The successful incorporation of the submicrometer-sized ZIF-71 into the PDMS membrane was also evidenced by ATR-IR and XRD characterizations (Supporting Information Figure S2,S3). The spectrum of pure ZIF-71 matches well with the pattern reported in the literature.[18d] The transmittance peaks at 665 cm−1 and 1055 cm−1 are assigned to the C–Cl and C–N vibrations of the imidazole ring, respectively (Figure S2).[18d] No apparent shifts in the bands were observed for the ZIF-71 filled PDMS membrane, indicating that there were no chemical interactions between the ZIF-71 particles and the polymer. The XRD patterns of the PDMS membrane and ZIF-71 filled PDMS membrane are presented in Figure S3. The PDMS membrane is completely amorphous,[29] whereas, the crystalline structure of ZIF-71 particle is preserved after incorporation for the ZIF-71 filled PDMS membrane (Figure S3b).
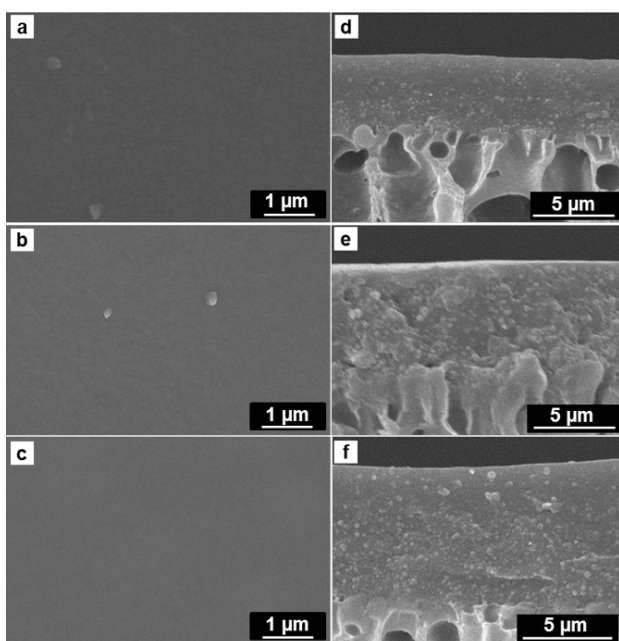

Figure 6.a–c) Top and d–f) cross-sectional views SEM images of submicrometer-sized ZIF-71 filled composite membranes prepared from 20% PDMS with different loadings a,d) 20 wt%, c,e) 30 wt%, and c,f) 40 wt%.

2.4 Pervaporation Performance

The development of energy-efficient and environmentally friendly separation processes has become an important and challenges exist in the development of sustainable and renewable energy such as CO_2 capture, natural gas and biofuel purification. Bioethanol is produced from biomass by fermentation.[30] However, microorganisms are generally inhibited by ethanol concentrations resulting in low productivity. Pervaporation with ethanol-selective membranes could be efficient approach to remove ethanol from diluted aqueous fermentation broths. Pervaporation can be described by the solution-diffusion transport model, following a three-step process: sorption-diffusion-desorption. The separation is thus based on the selective sorption and diffusion of components. The potential of submicrometer-sized ZIF-71 filled PDMS membrane with different MOF loadings (20–40 wt%) was studied for pervaparation separation of ethanol from a 5% ethanol aqueous solution at 50 °C using by a home-made set up (Supporting Information Figure S4). In order to correctly interpret the influence of ZIF-71 loading on the transport process, all membrane fluxes were normalized to 5 μm. The intrinsic permeability of the membranes was calculated by correcting for the driving force as shown in Figure 7. The submicrometer-sized ZIF-71 filled PDMS membranes display a gradual increase in separation factor and flux with increasing ZIF-71 loading (20–40 wt%) (Figure 7a,c). However, the separation factors of the micrometer-sized ZIF-71 filled membranes decrease at higher ZIF-71 loadings (Figure 7c). The results suggest that the submicrometer-sized ZIF-71 particles are better suited for the preparation of defect-free thin composite membranes. This was further confirmed by testing the pervaporation performance of thinner ZIF-71 filled membranes having thickness of 2.8 μm (Figure 5). The submicrometer-sized ZIF-71 filled membranes indeed showed a better pervaporation performance than the micro¬meter-sized ZIF-71 filled membranes (Supporting Information Figure S5). The remarkable effect of ZIF-71 in PDMS for significant improvements of flux and separation factor are due to the improved adsorption in the MOF as confirmed by the molecular simulation and FTIR spectroscopy analysis (vide infra Section 'Host–Guest Chemistry'). In addition, ZIF-71 has a micropore window of 0.48 nm which is larger than the kinetic diameter of ethanol (0.45 nm) and water (0.27 nm), thus the permeating molecules can diffuse more easily through the ZIF-71 than the dense membrane. The highest separation factor of 10.1 was achieved at 40 wt% loading for submicrometer-sized ZIF-71 filled membrane as compared to 7.6 for the micrometer-sized ZIF-71 filled membrane (Figure 7c). Under similar conditions, the pure PDMS membrane gave a separation factor of 5.8, as shown in Figure 7c. Moreover, our submicrometer-sized ZIF-71 PDMS membrane also outperformed the recently reported self-supported ZIF-71 membrane on ZnO substrate for 5% ethanol recovery at 25°C considering a lower flux (322.18 g m−2 h−1) and separation factor (6.07) were achieved.[18c].
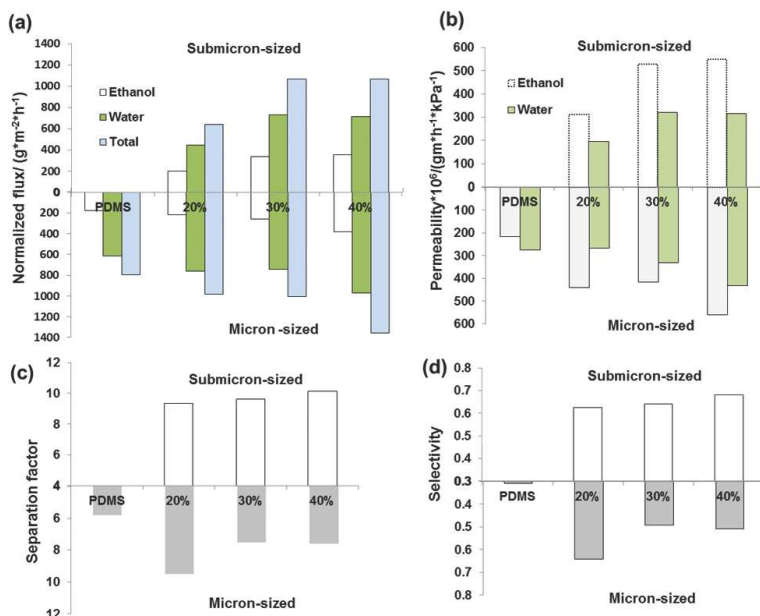
Figure 7. Comparison of the pervaporation performance a) flux normalized to 5 μm, b) permeability, c) separation factor, and d) selectivity of the micrometer-sized and submicrometer-sized ZIF-71 filled PDMS membranes prepared from 20% PDMS with different ZIF-71 loadings (20, 30, and 40 wt%). The data presented in the reverse order indicates the pervaporation results of the micrometer-sized ZIF-71 filled PDMS membranes. The pervaporation was run at 50 °C using 5% ethanol-water mixtures. The total flux and separation factor values were obtained based on average equilibrium performances of 3 different membrane coupons. The calculated standard deviations were 2–3%.

2.5 Host–Guest Chemistry

2.5.1 Grand Canonical Monte Carlo (GCMC) Simulation

Figure 8 shows the density contours of ethanol and water in ZIF-71 obtained from simulation at 0.1, 1, and 5 kPa, respectively. At 0.1 kPa, ethanol molecules are adsorbed in the six-membered rings and form clusters due to steric hindrance effect.[31] With increasing pressure to 1 kPa, adsorption starts to occur at the center of α-cages and prismatic cages. At 5 kPa, the α-cages are almost fully filled. For water, however, there is only negligible adsorption at low pressures (0.1 and 1 kPa) because of the intrinsic super-hydrophobicity of the ZIF-71 framework. Increasing pressure to 5 kPa, water clusters are formed in the six-membered rings. As observed, ethanol has a stronger adsorption capacity than water.
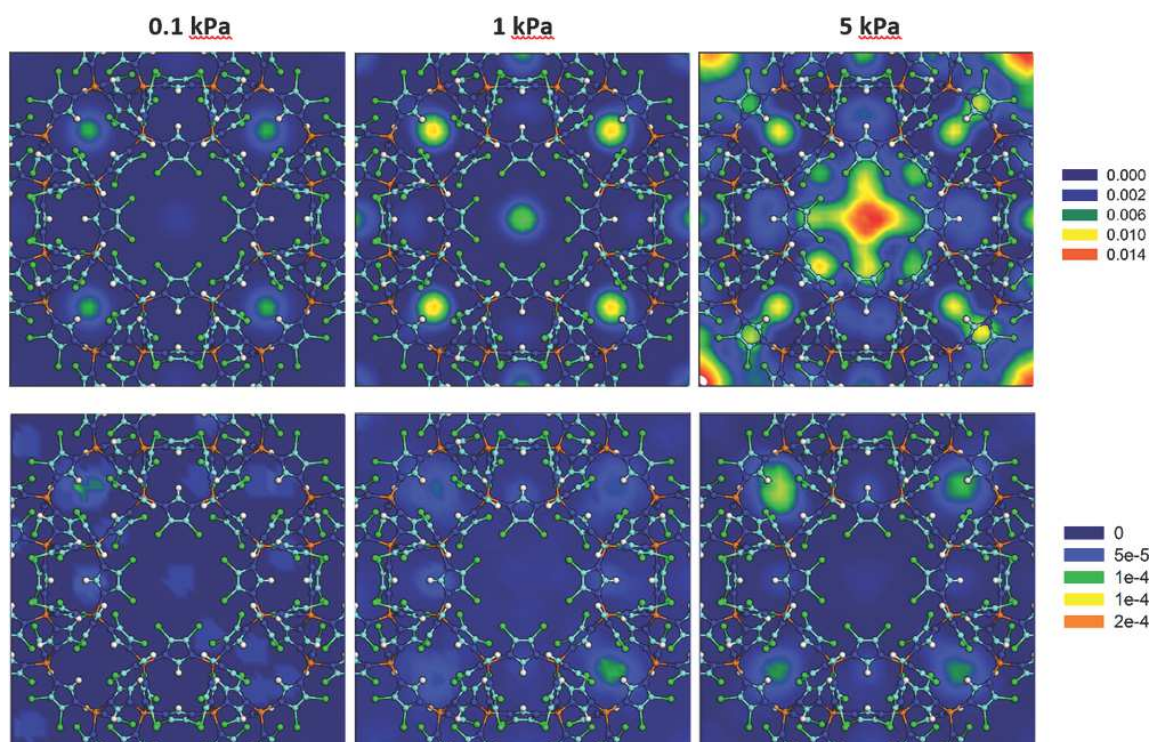
Figure8. Density contours of ethanol (top) and water (bottom) in ZIF-71 at 30 °C. The unit of density scale is the number of molecules per Å^3.

Figure 9 shows the density contours of ethanol-water mixtures in ZIF-71 obtained from simulation at different compositions of ethanol, XE = 5, 50, and 90%, respectively. The temperature and pressure considered are at ambient conditions (25 °C and 1 bar). At a low XE = 5%, ethanol in ZIF-71 is densely localized near –Cl atoms of the dcIm linker, indicating the favorable interaction between ethanol and the organic linker in the framework of ZIF-71 through induced adsorption-desorption isotherms and heats of adsorption.[32] Interestingly, a significant amount of water molecules are co-adsorbed, which is consistent with the experimental pervaporation data for flux (Figure 7a). Water molecules are saturated on the outer ring of adsorbed ethanol at the center of α-cages. The observed phenomenon of enhanced water uptake from ethanol-water could be due to the following reasons: i) the formation of terminal –NH monolayer on the crystal surface which favors hydrogen bonding with vapor-phase water,[25a] ii) the highly associative nature and small size of water which extends hydrogen bonding network and favors free-space filling[31] and iii) the tendency of ethanol to act as a seed to promote water adsorption.[32, 33] The simulated results well explain the experimentally observed water uptake in ZIF-71 filled MMMs. Upon increasing XE to 50%, the density of ethanol increases slightly at the cage center whereas water adsorption declines. At XE = 90%, the cage center is almost exclusively occupied by ethanol meanwhile water adsorption is largely reduced. Moreover, ethanol is also adsorbed in the six-membered rings and prismatic cages.
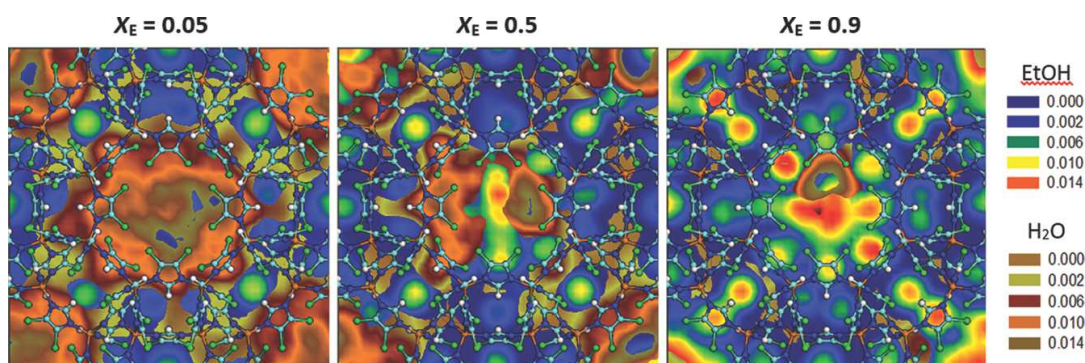
Figure 9. Density contours of ethanol-water mixtures in ZIF-71 at 25 °C and 1 bar. The unit of density scale is the number of molecules per Å^3.

2.5.2 FTIR Spectroscopy

Supporting Information Figure S6 reports a series of FTIR data collected in transmission mode on a thin ZIF-71 self-supporting pellet. The typical IR fingerprint of the ZIF-71 are clearly visible. Ethanol vapor pressure gives rise to the red curve as shown in Figure S6. The major effects of attributed to ethanol and ZIF-71 interaction are the band broadening and complex absorption in the region from 3700 to 2000 cm^{-1}. In particular a weak band at 3618 cm^{-1}, a second broader maximum centered at 3370 cm^{-1}, and a wide band superimposed to the framework ZIF-71 combination and overtone bands mixed with the ν(CH) of CH$_2$ and CH$_3$ of ethanol are observed. The effect of progressive outgassing are reported as grey curves (last spectrum was collected after 30 min of outgassing). It is clear that ethanol adsorption is only partially reversible and that the irreversible fraction of ethanol is characterized by hydrogen bonding interaction which are stronger than those observed in ethanol liquid-phase. For sake of clarity, dot dashed curve represents the spectrum of a thin film of liquid ethanol was collected. The direct comparison of the data allows the assignment the band at 3618 cm^{-1} to terminal ν(OH) of ethanol, while the maximum, centered at 3370 cm^{-1} to hydrogen bonded ethanol in the liquid form, respectively. The broad adsorption centered at 3000 cm^{-1} is persisted due to prolonged outgassing procedure and the direct interaction between ethanol and ZIF-71 wall cages.

3 Conclusion

Fine tuning of ZIF-71 crystal size and morphology from a simple mixed solvent approach is demonstrated in the absence of surfactant/modulator. The submicrometer-sized ZIF-71 crystals were ideal fillers for the fabrication of thin, smooth and homogeneous MMMs having a excellent filler dispersion for improving the pervaporation performance, outperformed the pure polymer membrane and micrometer-sized ZIF-71 filled MMMs. These submicrometer-sized ZIF-71 crystals with high permanent microporosity would also be useful, for example, as a seed layer for the preparation of thin films/membranes for other emerging applications such as chemical sensing and gas separation. The simulation and spectroscopy results gained insight on the molecular understanding for the significant role of the –Cl groups on the dcIm linker in the adsorption of ethanol within the cages of ZIF-71. These new findings are of paramount importance for future design and development of new nanoporous MOFs and open up the possibilities for further improvement of bioethanol recovery processes.

4 Experimental Section

Synthesis of Submicrometer-Sized ZIF-71: Submicrometer-sized ZIF-71 crystals were prepared by adding zinc acetate (0.74 g) and 4,5-dicholorimidazole (dcIm) (2.2 g) in methanol:DMF (2:1 = v/v) mixture (300 mL). The molar ratio of Zn:dcIm = 1:4. The solution was mixed under vigorous

magnetic stirring for 30 minutes and left static at room temperature for 24 h. The solvent was then removed and filled with chloroform (100 mL) and soaked for 2 days (2 × 100 mL). To recover the crystals, the solution was centrifuged and the chloroform was decanted. The crystals were then dried under vacuum at 100 °C for 24 h to remove any of the remaining solvents from the crystals. 80% yield of submicrometer-sized ZIF-71 was obtained based on Zn. Micrometer-sized ZIF-71 was prepared according to the recipe mentioned as above but methanol (300 mL) was used as a solvent.

Preparation of Submicrometer-Sized ZIF-71 Filled MMMs: Polyvinylidene fluoride (PVDF) ultrafiltration membranes were used as support. 20 wt% of PVDF in N-methyl-2-pyrrolidone (NMP) solutions was cast on a polypropylene non-woven support (Freudenberg, Germany) with a 200 μm casting knife and immersed in a room temperature water bath. The membranes were stored in water for two days and dried in air at room temperature. The ZIF-71 particles were dispersed in hexane by using a probe-type sonicator in an ice bath. The PDMS (RTV615A:RTV15B = 9:1) in hexane was pre-cross-linked at 60 °C for 2 h. The ZIF-71 solution was added into the pre-cross-linked PDMS solution to form 4, 5, and 20 wt% PDMS solutions in hexane and the solutions were sonicated for another 5 min. The ratio of PDMS to ZIF-71 in the solution was controlled at 20, 30, and 40 wt%. The composite membranes were prepared by coating the solutions on the PVDF support and were cross-linked at 110 °C. Part of the solutions were poored in a petri dish and cross-linked at 110 °C to form self-standing films for XRD and ATR-IR characterization.

Characterization Techniques: The as-synthesized ZIF-71 and films were characterized by a powder X-ray diffractometer (XRD) (STOE StadiP diffractometer in high-throughput transmission mode employing Cu $K_{\alpha}1$ radiation). The morphologies of ZIF-71 and membranes were characterized by a scanning electron microscope (SEM, Philips XL-30 FEG instrument equipped with a tungsten filament. Prior to analysis, sample was spread on carbon discs mounted to SEM aluminum pin stubs and gold sputtered. Attenuated total reflection infrared (ATR-IR, Bruker, Alpha) spectrophotometer was employed to investigate the surface chemistry of ZIF-71 and MMMs. The thermal stability of ZIF-71 was investigated by a thermo-gravimetric instrument (TGA, Q500) under nitrogen condition at a heating rate of 5 °C/min from room temperature to 800 °C. The particle size of the submicrometer-sized crystals was determined by a dynamic light scattering instrument (DLS-90 Plus Particle Size Analyzer, Brookhaven Instruments Corporation).

Pervaporation Separation of Ethanol-Water Mixture: Pervaporation experiments were carried out in a dead-end set-up (see Figure S4 in the Supporting Information). The dead-end cell has a feed volume of 1.5 L and an effective area of 12 cm^2. The pervaporation test was run at a constant temperature of 50 °C. The permeate sample was collected by a cold trap immersed in liquid nitrogen after stabilization for 2 h. 5 wt% of ethanol was chosen as feed to investigate the membrane performance. The concentration was measured by an Automatic Digital Refractometer (RX-7000α). Membrane flux and alcohol separation factor performance were calculated by the following, respectively:

$$J = \frac{W}{A \times \Delta t} \quad (1)$$

$$\beta = \frac{C_P/(1-C_P)}{C_F/(1-C_F)} \quad (2)$$

where, J is the flux, W is the weight of permeate sample, t is the collecting sample time, A is the membrane area, β is the separation factor, C_P is the ethanol concentration in the permeate and C_F the ethanol concentration in the feed. The intrinsic membrane properties are the permeability (P) and the selectivity which are defined as follows, respectively:

$$P_i = \frac{J_i \times l}{P_{i,\text{feed}}^{\text{vapor}} - n_{i,\text{permeate}} \times P_{\text{permeate}}} \quad (3)$$

$$\alpha_{i/j} = \frac{P_i / M_i}{P_j / M_j} \quad (4)$$

where, J_i is the permeation flux of component i, $P_{i,\text{feed}}^{\text{vapor}}$ is the equilibrium partial pressure of component i in the feed (kPa) calculated by software Aspen Plus, $n_{i,\text{permeate}}$ is the mole fraction of component i in the permeate side, P_{permeate} is the permeate side pressure (kPa), l the membrane thickness (m), P_i and P_j are the permeability of component i and j, (g m h^{-1} KPa^{-1}), M_i and M_j are the molecular weight of components.

Simulation Method: To provide a microscopic insight into adsorption behavior in ZIF-71, GCMC method was used to simulate the adsorption of pure ethanol and water as well as their mixtures.[34a] The atomic charges of ZIF-71 were calculated by density functional theory. In our recent study, three different force fields including UFF, DREIDING, and AMBER were tested for the adsorption of C1−C4 alcohols in ZIF-8; and DREIDING was found to exhibit the best agreement with experiment.[34b] Therefore, the dispersion interactions of ZIF-71 were described by DREIDING. Ethanol was represented by a united-atom model with each CHx as a single interaction site, and the potential parameters were adopted from TraPPE force field.[35] Water was mimicked by the three-point transferable potential model.[36] In the GCMC simulation, the Lennard-Jones interactions were evaluated with a spherical cut-off of 1.5 nm. For the Coulombic interactions, the Ewald sum with a tin-foil boundary condition was used. The real/reciprocal space partition parameter and the cut-off for reciprocal lattice vectors were chosen to be 0.02 nm−1 and 8, respectively, to ensure the convergence of the Ewald sum. The number of trial moves in a typical GCMC simulation was 2 × 107, in which the first half were used for equilibration and the second half for ensemble averages. Five types of trial moves were randomly attempted, namely displacement, rotation, partial regrowth at a neighboring position, complete regrowth at a new position, and swap between reservoir including creation and deletion with equal probability. To improve sampling efficiency, configurational-bias technique was adopted in which an adsorbate molecule was grown atom-by-atom biasing towards energetically favorable configurations while avoiding overlap with other atoms.[37] Specifically, the trial positions were generated with a probability proportional to $\exp\left(-\beta U_{\text{intra}}^i\right)$, where $\beta = 1/k_\beta T$ and U_{intra}^i is the intramolecular interaction energy at a position i. The numbers of trial positions for the first and subsequent atoms were fifteen and ten for pure ethanol and water, while twenty and fifteen for ethanol-water mixtures.

FTIR Spectroscopy: FTIR spectra were performed on ZIF-71 powders in the form of thin self-supporting pellet inserted into an homemade cell that allows in situ temperature activation at 300 °C under vacuum and FTIR spectra collection in presence of the desired equilibrium pressure of gaseous molecular probes. FTIR spectra were recorded on the activated sample at 2 cm^{-1} resolution, on a Nicolet 6700 spectrophotometer equipped with a liquid N_2 cooled MCT detector. The reported spectra refer to desorption experiments, where ethanol equilibrium pressure was reduced step by step by outgassing the cell, obtaining a sequence of spectra corresponding to decreasing coverage.

and the National University of Singapore. A typo in the article title was corrected on January 27, 2015.

References

[1] a) G. Ferey , *Chem. Soc. Rev.* **2008** , *37* , 191 ; b) V. Guillerm , D. Kim , J. F. Eubank , R. Luebke , X. Li , K. Adil , M. S. Lah , M. Eddaoudi ,*Chem. Soc. Rev.* **2014** , *43* , 6141 ; c) M. Li , D. Li , M. O'Keeffe , O. M. Yaghi , *Chem. Rev.* **2014** , *114* , 1343 .

[2] a) H. Furukawa , K. E. Cordova , M. O'Keeffe , O. M. Yaghi , *Science* **2013** , *341* , 974 ; b) J. A. Mason , M. Veenstra , J. R. Long , *Chem. Sci.***2014** , *5* , 32 ; c) L. J. Murray , M. Dincă , J. R. Long , *Chem. Soc. Rev.* **2009** , *38* , 1294 ; d) Z. R. Herm , B. M. Wiers , J. A. Mason , J. M. van Baten , M. R. Hudson , P. Zajdel , C. M. Brown , N. Masciocchi , R. Krishna , J. R. Long , *Science* **2013** , *340* , 960 ; e) B. Liu , M. Tu , D. Zacher , R. A. Fischer , *Adv. Funct. Mater.* **2013** , *23* , 3790 ; f) O. Shekhah , Y. Belmabkhout , Z. Chen ,V.Guillerm , A. Cairns , K. Adil , M. Eddaoudi , *Nat. Commun.* **2014** , *5* , 4228 ; g) Y. Peng , T. Gong , K. Zhang , X. Lin , Y. Liu , J. Jiang , Y. Cui , *Nat. Commun.* **2014** , *5* , 4406 .

[3] a) L. E. Kreno , K. Leong , O. K. Farha , M. Allendorf , R. P. Van Duyne , J. T. Hupp , *Chem. Rev.* **2012** , *112* , 1105 ; b) A. Corma , H. Garcia , F. X. Llabres i Xamena , *Chem. Rev.* **2010** , *110* , 4606 ; c) P. Garcia Garcia , M. Muller , A. Corma , *Chem. Sci.* **2014** , *5* , 2979 ; d) D. Farrusseng , S. Aguado , C. Pinel , *Angew. Chem., Int. Ed.* **2009** , *48* , 7502 .

[4] a) Z. Hu , B. J. Deibert , J. Li , *Chem. Soc. Rev.* **2014** , *43* , 5815 ; b) L. E. Kreno , K. Leong , O. K. Farha , M. Allendorf , R. P. Van Duyne , J. T. Hupp , *Chem. Rev.* **2012** , *112* , 1105 ; c) M. Meilikhov , S. Furukawa , K. Hirai , R. A. Fischer , S. Kitagawa , *Angew. Chem.* **2013** , *125* , 359 .

[5] a) P. Horcajada , R. Gref , T. Baati , P. K. Allan , G. Maurin , P. Couvreur , G. Ferey , R. E. Morris , C. Serre , *Chem. Rev.* **2012** , *112* , 1232 ; b) J. D. Rocca , D. Liu , W. Lin , *Acc. Chem. Res.* **2011** , *44* , 957 .

[6] L. H. Wee , S. R. Bajpe , N. Janssens , I. Hermans , K. Houthoofd , C. E. A. Kirschhock , J. A. Martens , *Chem. Commun.* **2010** , *46* , 8186 .

[7] K. M. Choi , H. M. Jeong , J. H. Park , Y.-B. Zhang , J. K. Kang , O. M. Yaghi , *ACS Nano* **2014** , *8* , 7451 ; b) Y.-S. Li , H. Bux , A. Feldhoff , G.-L. Li , W.-S. Yang , J. Caro , *Adv. Mater.* **2010** , *22* , 3322 ; c) G. Dong , H. Li , V. Chen , *J. Mater. Chem. A* **2013** , *1* , 4610 ; d) J. Gascon , F. Kapteijn , *Angew. Chem. Int. Ed.* **2010** , *49* , 1530 .

[8] a) N. Stock , S. Biswas , *Chem. Rev.* **2012** , *112* , 933 ; b) M. Oh , C. A. Mirkin , *Nature* **2005** , *438* , 651 ; c) W. Lin , W. J. Rieter , K. M. L. Taylor , *Angew. Chem. Int. Ed.* **2009** , *48* , 650 ; d) A. M. Spokoyny , D. Kim , A. Sumrein , C. A. Mirkin , *Chem. Soc.Rev.* **2009** , *38* , 1218 ; e) A. Carne , C. Carbonell , I. Imaz , D. Maspoch , *Chem. Soc. Rev.* **2011** , *40* , 291 ; f) E. A. Flugel , A. Ranft , F. Haase , B. L. Lotsch , *J. Mater. Chem.* **2012** , *22* , 10119 ; g) V. Valtchev , L. Tosheva , *Chem. Rev.* **2013** , *113* , 6734 ; h) M. Sindoro , N. Yanai , A.-Y. Jee , S. Granick , *Acc. Chem. Res.* **2014** , *47* , 459 .

[9] a) A. Schaate , P. Roy , A. Godt , J. Lippke , F. Waltz , M. Wiebcke , P. Behrens , *Chem. Eur. J.* **2011** , *17* , 6643 ; b) L.-T. Yang , L.-G. Qiu , S.-M. Hu , A. J. Xie , Y.-H. Shen , *Inorg. Chem. Commun.* **2013** , *35* , 265 ; c) M.-H. Pham , G.-T. Vuong , A.-T. Vu , T.-O. Do , *Langmuir* **2011** , *27* , 15261 ; d) S. Diring , S. Furukawa , Y. Takashima , T. Tsuruoka , S. Kitagawa , *Chem. Mater.* **2010** , *22* , 4531 ; e) K. M. L. Taylor , W. J. Rieter , W. Lin , *J. Am. Chem. Soc.* **2008** , *130* , 14358 ; f) W. J. Rieter , K. M. L. Taylor , H. An , W. Lin , W. Lin , *J. Am. Chem. Soc.* **2006** , *128* , 9024 ; g) Y. L. Liu , X. J. Zhao , X. X. Yang , Y. F. Li , *Analyst* **2013** , *138* , 4526 ; h) M. Ma , D. Zacher , X. Zhang , R. A. Fisher , N. Metzler-Nolte , *Cryst. Growth Des.* **2011** , *11* , 185 .

[10] a) S. H. Jhung , J. -H. Lee , J. W. Yoon , C. Serre , G. Ferey , J. -S. Chang , *Adv. Func. Mater.* **2007** , *19* , 121 ; b) S. M. F. Vilela , D. Ananias , J. A. Fernandes , P. Silva , A. C. Gomes , N. J. O. Silva , M. O. Rodrigues , J. P. C. Tome , A. A. Valente , P. Ribeiro-Claro , L. D. Carlos , J. Rocha , F. A. Almeida Paz , *J. Mater. Chem. C* **2014** , *2* , 3311 .

[11] M. Klimakow , P. Klobes , A. F. Thunemann , K. Rademann , F. Emmerling , *Chem. Mater.* **2010** , *22* , 5216 .

[12] D. Zacher , J. Liu , K. Huber , R. A. Fisher , *Chem. Commun.* **2009** , 1031.

[13] a) N. A. Khan , I. J. Kang , H. Y. Seok , S. H. Jhung , *Chem. Eng. J.* **2011** , *166* , 1152 ; b) J. Zhang , L. Sun , F. Xu , F. Li , H.-Y. Zhou , Y.-L. Liu ,Z. Gabelica , C. Schick , *Chem. Commun.* **2012** , *48* , 759 .

[14] Y. Zhou , B. Yan , *Inorg. Chem.* **2014** , *53* , 3456 .

[15] a) R. Banerjee , A. Phan , B. Wang , C. Knobler , H. Furukawa ,M. O'Keeffe , O. M. Yaghi , *Science* **2008** , *319* , 939 ; b) A. Phan , C. J. Doonan , F. J. Uribe-Romo , C. B. Knobler , M. O'Keeffe , O. M. Yaghi , *Acc. Chem. Res.* **2010** , *43* , 58 ; c) J. -P. Zhang , Y. -B. Zhang , J. -B. Lin , X. M. Chen , *Chem. Rev.* **2012** , *112* , 1001 .

[16] a) Q. Song , S. K. Nataraj , M. V. Roussenova , J. C. Tan , D. J. Hughes , W. Li , P. Bourgoin , M. A. Alam , A. K. Cheetham , S. A. Al-Muhtaseb , E. Sivaniah , *Energy Environ. Sci.* **2012** , *5* , 8359 ; b) Z. Xie , J. Yang , J. Wan , J. Bai , H. Yi , B. Yuan , J. Lu , Y. Zhang , L. Zhou , C. Duan , *Chem. Commun.* **2012** , *48* , 5977 ; c) T. Yang , T.-S. Chung , *J. Mater. Chem. A* **2013** , *1* , 6081 ; c) S. Basu , A. Cano-Odena , I. F. J. Vankelecom , *Sep. Purif. Technol.* **2011** , *81* , 31 ; d) M. He , J. Yao , Z.-X. Low , D. Yu , Y. Feng , H. Wang , *RSC Adv.* **2014** , *4* , 7634 ; L. S. Lai , Y. F. Yeong , K. K. Lau , M. S. Azmi , *Sep. Sci. Technol.***2014** , *49* , 1490 ; f) C. Sitprasert , F. Y. Wang , V. Rudolph , Z. H. Zhu , *Chem. Eng. Sci.* **2014** , *180* , 23 ; g) T. Li , Y. Pan , K.-V. Peinemann , Z. Lai , *J. Membr. Sci.* **2013** , *425–426* , 235 ; h) F. Cacho-Bailo , B. Seoane , C. Tellez , J. Caronas , *J. Membr. Sci.* **2014** , *464* , 119 ; i) J. Yao , H. Wang , *Chem. Soc. Rev.* **2014** , *43* , 4470 .

[17] a) H. Bux , F. Liang , Y. Li , J. Cravillon , M. Wiebcke , J. Caro , *J. Am. Chem. Soc.* **2009** , *131* , 16000 ; b) T.-H. Bae , J. S. Lee , W. Qiu , W. J. Koros , C. W. Jones , S. Nair , *Angew. Chemie. Int. Ed.* **2010** , *49* , 9863 ; c) A. J. Brown , J. R. Johnson , M. E. Lydon , W. J. Koros , C. W. Jones , S. Nair , *Angew. Chem. Int. Ed.* **2012** , *51* , 10615 ; d) A. Huang , N. Wang , C. Kong , J. Caro , *Angew. Chem. Int. Ed.* **2012** , *51* , 10551 ; e) J. A. Gee , J. Chung , S. Nair , D. S. Sholl , *J. Phys.Chem. C* **2013** , *117* , 3169 ; f) A. Huang , Y. Chen , N. Wang , Z. Hu , J. W. Jiang , J. Caro , *Chem. Commun.* **2012** , *48* , 10981 .

[18] a) B. Zornoza , C. Tellez , J. Coronas , J. Gascon , F. Kapteijn , *Micropor. Mesopor. Mater.* **2013** , *116* , 67 ; b) X. -L. Liu , Y. -S. Li , G. -Q. Zhu ,Y. -J. Ban , L. -Y. Xu , W. -S. Yang , *Angew. Chem. Int. Ed.* **2011** , *50* ,10636 ; c) X. Dong , Y. S. Lin , *Chem. Commun.* **2013** , *49* , 1196 ; d) S. Liu , G. Liu , X. Zhou , W. Jin , *J. Membr. Sci.* **2013** , *446* , 181 ; e) D. Hua , Y. K. Ong , Y. Wang , T.-S. Chung , *J. Membr. Sci.* **2014** , *453* , 155 ; f) H. Fan , Q. Shi , H. Yan , S. Ji , J. Dong , G. Zhang , *Angew.Chemie Int. Ed.* **2014** , *53* , 5578 ; g) Y. Li , L. H. Wee , J. A. Martens ,I. F. J. Vankelecom , *J. Mater. Chem. A* **2014** , *2* , 10034 .

[19] a) J. Cravillon , R. Nayuk , S. Springer , A. Feldhoff , K. Huber ,M. Wiebcke , *Chem. Mater.* **2011** , *23* , 2130 ; b) J. Cravillion ,S. Munzer , S.-J. Lohmeier , A. Feldhoff , K. Huber , M. Wiebcke , *Chem.Mater.***2009** , *21* , 1410 ; c) X. Wang , P. Huang , P. Yu , L. Yang , L. Mao ,*ChemPlusChem* **2014** , *79* , 907 ; d) J.Cravillon , C. A. Schroder ,R. Nayuk , J. Gummel , K. Huber , M. Wiebcke , *Angew. Chem. Int. Ed.* **2011** , *123* , 8217 ; e) S. K. Nune , P. K. Thallapally , A. Dohnalkova ,C. Wang , J. Liu , G. J. Exarhos , *Chem.Commun.* **2010** , *46* , 4878 ;f) Y. Pan , Y. Liu , G. Zheng , L. Zhao , Z. Lai , *Chem. Commun.* **2011** 2071 ; g) S. R. Venna , J. B. Jasinski , M. A. Carreon , *J. Am. Chem. Soc.***2010** , *132* , 18030 ; h) L. H. Wee ,T. Lescouet , J. Ethiraj , F. Bonino ,R. Vidruk , E. Garrier , D. Packet , S. Bordiga , D. Farrusseng ,M. Herskowitz , J. A. Martens , *ChemCatChem* **2013** , *5* , 3562 ; i) B. Chen , F. Bai , Y. Zhu , Y. Xia , *Microporous Mesoporous Mater.* **2014** , *193* , 7 .

[20] a) T. Li , Y. Pan , K. -V. Peinemann , Z. Lai , *J. Membr. Sci.* **2013** , *425–426* , 235 ; b) X. Wang , P. Huang , P. Yu , L. Yang , L. Mao , *ChemPlusChem* **2014** , *79* , 907 ; c) Y. -S. Li , H. Bux , A. Feldhoff , G. -L. Li , W. -S. Yang , *Adv. Mater.* **2010** , *22* , 3322 .

[21] a) M. E. Schweinefus , S. Springer , I. A. Baburin , T. Hikov , K. Huber , S. Leoni , M. Wiebcke , *Dalton Trans.* **2014** , *43* , 3528 ; b) S. Japip , H. Wang , Y. Xiao , T. S. Chung , *J. Membr. Sci.* **2014** , *467* , 162 .

[22] J. Qian , F. Sun , L. Qin , *Mater. Lett.* **2012** , *82* , 220 .

[23] T. Yang , T. -S. Chung , *J. Mater. Chem. A* **2013** , *1* , 6081 .

[24] I. Persson , *Pure Appl. Chem.* **1986** , *58* , 1153 .

[25] a) R. P. Lively , M. E. Dose , J. A. Thompson , B. A. McCool , R. R. Chance , W. J. Koros , *Chem. Commun.* **2011** , *47* , 8667 ; b) K. Zhang , R. P. Lively , M. E. Dose , A. J. Brown , C. Zhang , J. Chung , S. Nair , W. J. Koros , R. R. Chance , *Chem. Commun.* **2013** , *49* , 3245 ; c) W. Morris , B. Leung , H. Furukawa , O. K. Yaghi ,N. He , H. Hayashi , Y. Houndonougbo , M. Asta , B. B. Laird , O. M. Yaghi , *J. Am. Chem. Soc.* **2010** , *132* , 11006 ; d) H. Fei , J. F. Cahill , K. A. Prather , S. M. Cohen , *Inorg. Chem.* **2013**, *52* , 4011 .

[26] a) X. Cheng , A. Zhang , K. Hou , M. Liu , Y. Wang , C. Song , G. Zhang , X. Guo , *Dalton Trans.* **2013**, *42* , 13698 ; b) E. L. Bustamante , J. L. Fernandez , J. M. Zamano , *J. Colloid Interface Sci.* **2014** , *424,* 37 .

[27] a) A. Schejn , L. Balan , V. Falk , L. Aranda , G. Medjahdi , R. Schneider , *CrystEngComm* **2014** , *16* , 4493; b) J. Cravillon , C. A. Schroder ,H. Bux , A. Rothkirch , J. Caro , M. Wiebcke , *CrystEngComm* **2012** , *14* ,492.

[28] a) V. Dusastre , *Nat. Mater.* **2013** , *12* , 778 ; b) R. Ameloot, E. Gobechiya , H. Uji-I , J. A. Martens , J. Hofkens , L. Alaerts ,B. F. Sels , D. E. De Vos , *Adv. Mater.* **2010** , *22* , 2685 ; c) S. Li , G. Lu , X. Huang H. Li , Y. Sun , H. Zhang , X. Chen , F. Huo , *Chem. Commun.* **2012** , *48* , 11901 ; d) D. Witters , N. Vergauwe , R. Ameloot, S. Vermeir , D. DeVos , B. Puers , B. Sels , J. Lammertyn , *Adv. Mater.* **2012** , *24* , 1316 .

[29] B. Li , D. Xu , Z. Jiang , X. Zheng , W. Liu , X. Dong , *J. Membr. Sci.***2008** , *322* , 293 .

[30] N. L. Le , Y. Wang , T.-S. Chung , *J. Membr. Sci.* **2011** , *379* , 174 .

[31] A. Nalaparaju , X. S. Zhao , J. W. Jiang , *J. Phys. Chem. C* **2010** , *114* ,11542 .

[32] K. Zhang , A. Nalaparaju , Y. Chen , J. Jiang , *Phys. Chem. Chem. Phys.,* **2014** , *16* , 9643 .

[33] A. U. Ortiz , A. P. Freitas , A. Boutin , A. H. Fuchs , F.-X. Coudert , *Phys. Chem. Chem. Phys.* **2014** , *16* , 9940 .

[34] a) N. Nalaparaju , X. S. Zhao , J. W. Jiang , *Energy Environ. Sci.* **2011** , *4* , 2107 ; b) K. Zhang , L. Zhang , J. Jiang , *J. Phys. Chem. C* **2013** , *117* , 25628 .

[35] B. Chen , J. J. Potoff , J. I. Siepmann , *J. Phys. Chem. B* **2001** , *105* , 3093.

[36] W. L. Jorgensen , J. Chandrasekhar , J. D. Madura , R. W. Impey , M. L. Klein , *J. Chem. Phys.* **1983** , *79* , 926 .

[37] a) D. Frenkel , G. C. A. M. Mooij , B. Smit , *J. Phys.: Condensed Matter.* **1992** , *4* , 3053 ; b) J. J. De Pablo , M. Laso , U. W. Suter , *J. Chem. Phys.* **1992** , *96* , 2395 ; c) T. J. H. Vlugt , R. Krishna , B. Smit , *J. Phys. Chem. B* **1999** , *103* , 1102 .